Magnetic reversal in Mn5Ge3 thin films: an extensive study

L. Michez, A. Spiesser, M. Petit, S. Bertaina, J.F. Jacquot, Didier Dufeu, C. Coudreau, M. Jamet, Thanh V. Le

Magnetic reversal in Mn_5Ge_3 thin films: An extensive study

L.-A. Michez,[1,*] A. Spiesser,[1,†] M. Petit,[1] S. Bertaina,[2] J.-F. Jacquot,[3] D. Dufeu,[4] C. Coudreau,[1] M. Jamet,[3] and V. Le Thanh[1]

[1] *Aix Marseille Université, CNRS, CINaM-UMR 7325, 13288, Marseille, France*
[2] *Aix-Marseille Université , CNRS, IM2NP-UMR 6242, 13397, Marseille, France*
[3] *CEA-Grenoble, INAC/SP2M, Grenoble, France*
[4] *Institut Néel, 38042 Grenoble, France*

(Dated: November 21, 2014)

We present a comprehensive study of magnetization reversal process in thin films of Mn_5Ge_3. For this investigation, we have studied the magnetic anisotropy of Mn_5Ge_3 layers as a function of the film thickness using VSM and SQUID magnetometers. The samples grown by molecular beam epitaxy exhibit a reorientational transition of the easy axis of magnetization from in-plane to out-of-plane as the film thickness increases. We provide evidences that above a critical thickness estimated to 20 nm, the magnetic structure is constituted of stripes with out-of-plane magnetization pointing alternatively up and down. We have analyzed our results using different phenomenological models and all the calculations converge towards values for magnetocrystalline anisotropy constant and saturation magnetization that are in excellent agreement with the reported values for bulk Mn_5Ge_3. This study has also lead to the first estimation in Mn_5Ge_3 of the exchange constant, the surface energy of domain walls as well as their width. These parameters are essential for determining whether this material can be used in the next generation of spintronic devices.

PACS numbers: 77.80.Dj, 75.60.Jk, 75.50.Cc, 75.30.Gw

I. INTRODUCTION

The ferromagnetic compound Mn_5Ge_3 holds great promise for novel devices and this material is under investigation in emerging topics such as spintronics[1–3] and magnetocaloric effect.[4,5] The major attractive feature of this material stems from its high compatibility with the already-existing silicon-based technology since it can be epitaxially grown on germanium (Ge) with very high crystalline quality.[6] Mn_5Ge_3 is particularly attractive to promote semiconductor spintronics, which is believed to constitute one of the promising solutions to develop the beyond complementary metal-oxide-semiconductor technology.[7] The Mn_5Ge_3 compound presents indeed all the prerequisite criteria necessary in spin electronics: high Curie temperature (> 296K) that can be enhanced up to 420K by adding a small amount of carbon (C)[8], reasonable spin polarization[9,10], very high crystal quality and sharp interface with Ge(111)[11,12] which allows direct electrical transport between the ferromagnet and the conduction band of Ge via tunneling through the Schottky barrier without the need of an insulating barrier.[13] This approach makes the realization of gate-tunable spin devices conceivable and simplifies both technological implementation and theoretical modeling. As further advantages, its perpendicular magnetic uniaxial anisotropy is of particular interest because of potential applications in both spintronics and magnetic recording.[14] It has to be noted that conventional materials with perpendicular magnetic anisotropy such as Co and Co-based alloys are not directly compatible with Si or Ge-technologies as they are prone to form non-ferromagnetic interfacial compounds. Accordingly, Mn_5Ge_3 is a unique candidate for applications in both emerging Si-Ge spin-based electronics and next-generation of data storage.

Applications of ferromagnetic materials, such as data storage or spintronics devices are achieved through the control and manipulation of the domain structures, each of them being a nanoscale region with uniform spontaneous magnetization. In a recent paper,[15] we have demonstrated the presence of a critical thickness in Mn_5Ge_3 thin films below which the hysteresis loops are characteristic of samples having their magnetization confined in the sample plane. Above this critical thickness, the magnetization curves reveal the presence of a domain stripe structure in which the magnetization is perpendicular to the film plane. However, an extensive study is still lacking in order to fully characterize the process of magnetization reversal in Mn_5Ge_3 thin films. Consequently, this systematic study over a broad range of thicknesses aims at identifying and quantifying the various contributions leading to magnetic anisotropy in Mn_5Ge_3 thin films. A detailed investigation of the magnetic behavior of Mn_5Ge_3 layers below the critical thickness has been first carried out, followed by a thorough analysis of the multidomain structure. Using phenomenological models, we have determined the values of magnetic quantities such as the saturation magnetization, the magnetocrystalline anisotropy constant and the exchange constant and estimated domain wall characteristics. A more accurate value for the critical thickness has been determined. At last, the study of the angular dependence of the magnetization reversal allows us to provide for the first time a comprehensive description of the domain structure in Mn_5Ge_3 thin layers. This is a determinant step to test the potential of Mn_5Ge_3 as new material for the next-generation of spin-based devices.

II. FILM GROWTH AND EXPERIMENTAL TECHNIQUES

Mn_5Ge_3 films with thickness varying from 4 nm to 200 nm were grown in a Molecular Beam Epitaxy (MBE) system via solid phase epitaxy (SPE) which consists of a room temperature Mn deposition followed by thermal annealing at $\approx 450°C$ to activate interdiffusion and phase nucleation. The samples were then capped with amorphous Ge for *ex situ* characterizations. Detailed description of sample preparation and growth conditions are reported elsewhere.[11,16]

Structural properties of Mn_5Ge_3 thin films have been extensively studied using reflection high energy electron diffraction, Auger electron spectroscopy, high-resolution transmission electron microscopy techniques.[11,15] These measurements reveal a very high-quality crystalline heterostructure with a two-dimensional surface and a sharp interface between Mn_5Ge_3 and Ge(111) throughout all the considered range of thicknesses. Further analyses of post-grown films were performed by means of X-ray diffraction (XRD). A typical $\theta - 2\theta$ diffraction scan is shown in Fig.1 and displays only the (0002) and (0004) reflections of the Mn_5Ge_3 phase. The width at half maximum height of the first reflection has been measured to be 0.116°. Considering the broadening induced by the low thickness of the Mn_5Ge_3 film, this value is very close to the Ge(111) width at half maximum, which confirms the high crystalline quality of the structure. XRD also indicates that the (0001) Mn_5Ge_3 c-axis is parallel to the Ge(111) direction. No residual Mn has been detected, which means that all the deposited Mn has reacted to form a single crystalline phase. Worth noting, although the orthorhombic $Mn_{11}Ge_8$ phase is at equilibrium the most stable phase of the Mn-Ge phase diagram, Mn_5Ge_3 is the single compound present in our films and its stabilization results from similarities in the crystal symmetry between Mn_5Ge_3 and the pseudo-hexagonal Ge(111). All the characterization techniques also indicate that the films appear totally relaxed even for layers as thin as 1 nm.

The magnetic measurements discussed below were carried out with conventional magnetometers, i.e. an Oxford instruments vibrating sample magnetometer (VSM), a Quantum Design SQUID (superconducting quantum interference device magnetometer) and a Quantum Design SQUID-VSM in a temperature range varying from 5 to 320 K. The field dependence of the magnetic moments were measured in magnetic fields up to 2 T applied both parallel and perpendicular to the sample plane. The diamagnetic contribution coming from the Ge substrate was subtracted in the measurements presented below, leaving only the magnetic signal coming from the Mn_5Ge_3 films. Mn_5Ge_3 thicknesses considered in this study for the magnetization calculation correspond to the magnetically active part of the sample, which implies that the magnetic dead layer thickness that had been estimated to 1.7 ± 0.3 nm,[15] has been subtracted to the overall alloy thickness measured by TEM.

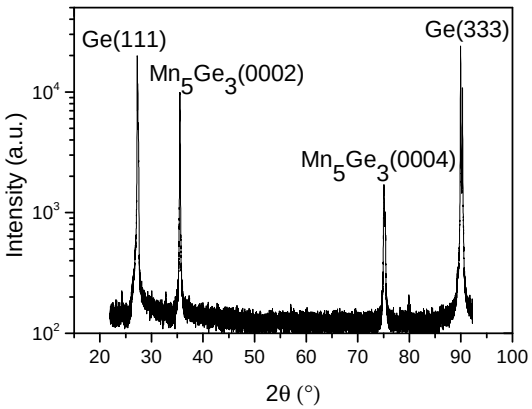

FIG. 1: XRD spectrum of a 70nm thick Mn_5Ge_3 film epitaxially grown on Ge(111) in the $\theta - 2\theta$ geometry.

III. EXPERIMENTAL RESULTS

The limited value of the Curie temperature (296K) of Mn_5Ge_3 prevents the direct observation of the domain structure by magnetic force microscopy (MFM) at room temperature. First clues about the magnetic structure have been presented in a previous paper[15] where the presence of two thickness ranges, each one corresponding to a well-defined magnetization orientation in the Mn_5Ge_3 thin films, have been demonstrated. Below a critical thickness, the magnetization lies in the sample plane. As the film thickness increases, a reorientation of the magnetization direction from in-plane to out-of-plane occurs and the films present a stripe-domain structure with Bloch-type domain walls (DWs). Within the domains, the magnetization is oriented perpendicularly to the surface and therefore lies along the c-axis of the Mn_5Ge_3 crystal as predicted in bulk samples.[17] This transition occurs for a film thickness lying between 10 and 25 nm and is the result of competing anisotropy mechanisms.

In this paper, an extensive study of the magnetization reversal as a function of the thickness is carried out with the objectives of providing useful information about the competing mechanisms giving rise to the magnetic anisotropy and the ability to form a domain structure.

A. Magnetic anisotropy in thin films

We first investigate the magnetic properties of the samples corresponding to the low-range thicknesses. Fig. 2 shows hysteresis loops of 2.5 nm-, 7 nm- and 11.5 nm- thin films measured at 15 K for magnetic field applied both in the sample plane and perpendicularly to it. For thicknesses less than 10 nm, the typical square

hysteresis loop in the in-plane measurement and the presence of a hard axis in the out-of-plane measurement clearly indicate an in-plane easy axis of magnetization. The magnetization of the film is therefore dominated by the magnetostatic anisotropy. For a single-domain film, the energy density contains contributions from the demagnetizing field, the uniaxial anisotropy and the Zeeman energy. The effective anisotropy K_{eff} of this monodomain film can be defined as the area between the perpendicular and the parallel magnetization curves. According to a phenomenological approach described by Gradmann,[18] one can express the effective anisotropy as $K_{eff} = K_u + K_s/d - 4\pi M_s^2$ where K_s and K_u are respectively the surface and uniaxial volume anisotropy and the last term represents the magnetostatic anisotropy. The magnetoelastic anisotropy has been neglected in this model since the films are relaxed from the first monolayers.[11] Considering the value of saturation as the bulk value,[17] we can determine the value of the uniaxial anisotropy and the surface energy to be respectively $(4.5 \pm 0.1) \times 10^6$ erg/cm^3 and (0.10 ± 0.04) erg/cm^2 at 15 K. The first value agrees very well with the bulk anisotropy constant[17] and is comparable to the one found in hexagonal Co films.[19] On the other hand, the surface anisotropy constant is much lower than the one found in hexagonal Co films.[20] This partly explains why the critical thickness is much smaller in Mn_5Ge_3 than in Co in which the surface anisotropy contributes significantly to the effective anisotropy. As a result, the quality factor Q defined as $Q = \frac{K_u}{2\pi M_s^2}$ is evaluated to 0.6 in Mn_5Ge_3 thin films. This is consistent with the theory developed for materials with uniaxial perpendicular anisotropy:[21] when $Q < 1$, a domain structure with an out-of-plane component of magnetization is present above a critical thickness t_c due to the instability of the magnetization direction.[22] As a result, the magnetization points alternatively in and out of the sample plane creating a stripe structure whereas it lies in the sample plane for lower thicknesses. Such a configuration has been observed in other systems like, for example, in Co[23] and FePd thin films,[24,25] but in both cases, the critical thickness is much higher. On the other hand, for the Mn_5Ge_3 system, changes in the shape of the hysteresis curves that reflect modifications of the magnetic structure can actually be observed for thicknesses as low as 10 nm. This is particularly visible in the in-plane magnetization curve shown in Fig.2c where the coercivity starts to increase and the curve becomes more canted due to an increase of the saturation field. This gradual change in $M - H$ is attributed to the fact that for materials with perpendicular anisotropy, the magnetization ought to switch out of the plane.

This reorientation is not unique and has been described by Saito for strong perpendicular anisotropy systems in NiFe thin films.[26,27] The in-plane magnetization configuration is no more energetically favorable and a small perpendicular component starts to grow above a critical

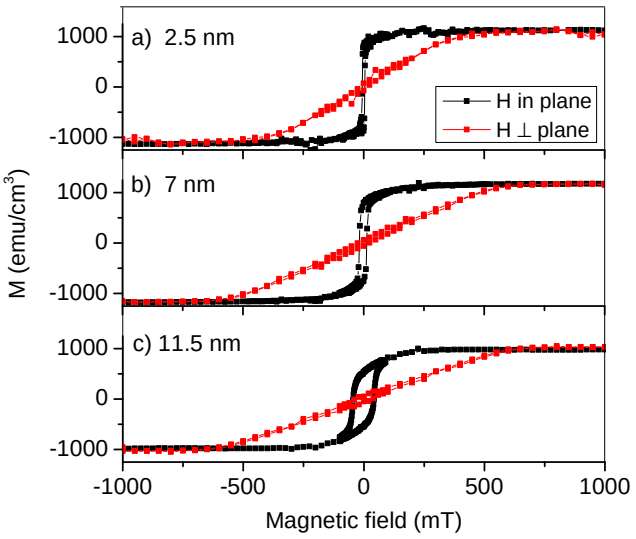

FIG. 2: (color online) Hysteresis loops performed at 15 K for (a)for 2.5nm, (b) 7nm and (c) 11.5nm thick samples with the external magnetic field applied in the sample plane (black squares) and perpendicular to it (red triangles).

thickness estimated to be $t_{c_1} = 27\left(\frac{8}{\pi^2}\right)^2 \sqrt{\frac{A M_{Sat}{}^4}{K^3}}$ where A is the exchange constant, M_{Sat} the saturation magnetization and K the uniaxial magnetocrystalline anisotropy. Substituting the values found above for M_{Sat} and K, the exchange constant can be estimated as $(2.2 \pm 0.5) \times 10^{-7}$ erg/cm which is in good agreements with the 1×10^{-7} erg/cm-value found previously.[15] It has to be noted that the exchange constant is considerably smaller than in hcp Co, which also explains the lower critical thickness in the present case. As the film thickness increases, the magnetization tends to be more and more perpendicular to the sample plane, corresponding to a decrease of the in-plane component of the magnetization while the domain structure becomes more pronounced. This structure ought to turn into stripe domains having full perpendicular anisotropy above a second critical thickness denoted as t_{c_2}.[21] The study of the magnetization reversal as a function of thicknesses over a broader range is therefore essential to determine the thickness dependence of the magnetic domain structure.

B. Magnetic anisotropy in thick films

1. *Thickness dependence of magnetic parameters*

Hysteresis curves of samples with a thickness varying up to 200 nm were recorded with the external magnetic field applied both parallel and perpendicular to the film plane. Fig.3 presents a summary of the thickness dependence of the saturation field, the coercive field and the

remanent magnetization.

We first focus on the thickness dependence of the coercive field (H_c), defined as the half width of the hysteresis loops. In both parallel and perpendicular configurations, H_c first displays a sharp increase until the critical value of 20 nm and then it decreases monotonously and reaches a limit value around 20 mT as shown in Fig. 3a. We can conjecture that the two effects are correlated and can be due to the transition from in-plane to perpendicular magnetization. Indeed, a large number of magnetic domain walls appears above the critical thickness and these walls may be responsible for a far larger coercivity through pinning to the interfaces or other defects. After the transition, the domain size increases reducing therefore the importance of the domain walls zone acting as pinning areas and contributing to the high value of the coercive field. Accordingly, we can deduce that the structure with perpendicular magnetic anisotropy domains is fully formed from 20 nm.

Using the Kittel's model[21] predicting that the critical thickness for which the easy axis of magnetization turns fully from an in-plane direction to the out-of-plane domain structure is $t_{c_2} \approx 6.8\sigma_w(\frac{M_{Sat}}{K_u})^2$ where σ_w is the wall energy, M_{Sat} the saturation magnetization and K_u the uniaxial magnetocrystalline anisotropy, we can estimate the wall energy to be about (5 ± 1) erg/cm^2. Two well-defined thickness ranges corresponding to different magnetic structure can therefore be identified. Up to 10 nm, the magnetostatic anisotropy forces the magnetization in the sample plane. Above 20 nm, the magnetization is out-of-plane in a stripe domain structure. The reorientation transition occurs gradually between these two critical values.

The 20 nm-thickness threshold is also clearly visible in the plot of the saturation field (H_{Sat}) defined as the field at which the magnetization reaches its saturation value M_s. As displayed in Fig. 3b, the saturation in the perpendicular configuration $H_{Sat\perp}$ first increases rapidly up to 20 nm, then increases gradually and saturates towards 11 kOe for the thickest films. In the transition region, the stripe structure is progressively constituted, leading to Bloch-type domain wall formation. As a result, a greater perpendicular field is necessary to overcome the in-plane magnetization component induced by the DWs. In samples with thicknesses above 20 nm, only the domain size is modified and the perpendicular saturation field slightly changes. A typical out-of-plane hysteresis curve corresponding to the higher-bound of the studied film thicknesses is displayed in Fig. 4b. The $M-H$ curve slope remains nearly constant from zero up to $H_{Sat}^{\perp}$, which results from the competition between magnetic pressures acting on the walls. Various models are available for describing the dependence of the saturation field on the film thickness and the best fit to our data is obtained with the Thiele's model,[28] which is particularly adapted to materials with uniaxial anisotropy exhibiting weak stripe structure. This model describes the magnetic state near perpendicular saturation in which bubble shape domains are far from each other and can therefore be considered as independent. From this model, the perpendicular saturation field is equal to $H_{Sat}^{\perp} = 4\pi M_{Sat}\left(1 - 1.596\sqrt{\frac{l}{t}}\right)$ with $l = \frac{\sigma_w}{4\pi M_{Sat}^2}$ where t is the film thickness and l a free parameter defined as a characteristic material length. The best fit, shown in Fig.3b, gives a saturation magnetization equal to 1040 emu/cm^3 and a wall surface energy of 2 erg/cm^2. The first value is in excellent concord with all the experimental measurements[17,29] whereas the latter reasonably agrees with the value determined previously from Kittel's model, especially as Bloch wall energy generally decreases with increasing the film thickness.[30] This result is also consistent with the general calculation of a Bloch-type domain wall energy: $\sigma_w = 4\sqrt{AK} \approx 4$ erg/cm^2.[31] At last, the wall width of a Bloch DW, theoretically given by $\Delta = \pi\sqrt{\frac{A}{K}}$[32] can be estimated to 7 nm in a 20 nm-thick Mn_5Ge_3 film. This value is in excellent agreement with theoretical calculations based on an improved version of the Kittel's model.[15]

The saturation field in the parallel configuration ($H_{Sat}^{//}$) follows a similar trend as $H_{Sat}^{\perp}$, but tends to a lower limit value of 0.85 T. In this geometry, walls are not submitted to a magnetic pressure from the magnetic field, and therefore, a coherent rotation is responsible of the magnetization reversal as shown in the typical in-plane $M-H$ curve displayed in Fig. 4b. Using a Stoner-Wohlwarth-type model to analyze our data, the saturation field in the parallel orientation can be described by the expression $H_{Sat}^{//} = 2K_u/M_{Sat} - H_{d^{\perp}}$ where $H_{d^{\perp}}$ is the thickness dependent perpendicular demagnetizing field. However, in our case, the domain structure is constituted of stripes. As a result, the demagnetizing field is equal to $4\pi N_{\perp} M_{Sat}$ where $N_{\perp}$ is the demagnetizing factor. Using for K_u and M_{Sat} the values found above, we demonstrate that $H_{d^{\perp}}$ is negligible to fit the experimental value. This suggests the presence of magnetic domains of sufficiently small aspect ratio favorable to decrease the demagnetization field to values close to zero. This result agrees very well with theoretical calculations based on an improved version of the Kittel's model for stripe domains developed for Mn_5Ge_3 thin films.[15] In this model, the domain wall's width first decreases rapidly with increasing film thickness and from a thickness of about 20nm it is rather independent of the film thickness whereas the size of a half stripe period corresponding to a domain wall and a domain width linearly increases with thickness (inset of Fig. 5 in Ref.15). The aspect ratio of domains varies therefore with the film thickness and the change is particularly visible for thicknesses under 20 nm. It implies that the demagnetizing field cannot be neglected for the low-range thicknesses, which leads to a decrease of $H_{Sat}^{//}$.

This stripe model conceived to describe magnetic structure in uniaxial anisotropy materials[33] can also be used to predict the thickness dependence of the in-plane remanent magnetization. When the magnetic field is switched off after saturation in an in-plane direction, the

magnetic moments of each DW are oriented along this very same direction. Consequently, the remanent magnetization corresponds only to the DWs in-plane contribution, which can easily be extracted from the model. The best fit of the experimental data has been obtained for an exchange constant of 1×10^{-7} erg/cm,[15] which agrees with the value obtained in section III A from the phenomenological model developed for samples with monodomain-type structure.

The remanent magnetization after perpendicular saturation is almost null over the whole range of thicknesses that we have studied. This originates from the domain structure, which is constituted of a stripe-type structure. Within consecutive domains, the magnetization is oriented in opposite direction along the c-axis leading therefore to almost null total magnetization.

To conclude this section, we have demonstrated that an extensive study of the in-plane and out-of-plane M-H curves reinforces the previous study of the reorientation of the magnetization in thin Mn_5Ge_3 films. The transition thickness has been determined more precisely and estimations for exchange constant, wall energy and magnetocrystalline anisotropy constant have been determined. It is worth noting that various independent models have been used to fit the different sets of data and they all give consistent results. However, a study of the magnetization reversal as a function of angle is still required in order to separate the various contributions of the competing sources of anisotropy and get a full comprehensive picture of the magnetization reversal in Mn_5Ge_3 thin films.

2. *Angle dependence of magnetic parameters*

Angle dependent measurements are in principle a valuable method to obtain a good insight into the magnetization process since direct comparisons can be made, revealing therefore fundamental mechanisms, such as coherent rotation, domain wall nucleation or pinning. We will only focus on films exhibiting a stripe domain structure since in the case of thin film with easy axis of magnetization lying in the sample plane, only magnetocrystalline and magnetostatic anisotropies and Zeeman energy compete to give rise to the magnetization orientation. As a result, one expects a coherent rotation during the magnetization reorientation.

To gain insight into the magnetic reversal process of films in the high-thickness range, in-plane and out-of-plane angular dependence of a 160 nm-thick film are shown in Fig.4. The measurements have been carried out at 5 K in an external magnetic field of 0.5 T, which is an intermediate value between coercive and saturation fields. First, the angle θ between the applied magnetic field and the sample plane is varied from 0° to 180°. A strong two-fold symmetry induced by the magnetocrystalline anisotropy is clearly visible in the perpendicular orientation. A weak in-plane anisotropy has also been observed by rotating the applied field within the sample

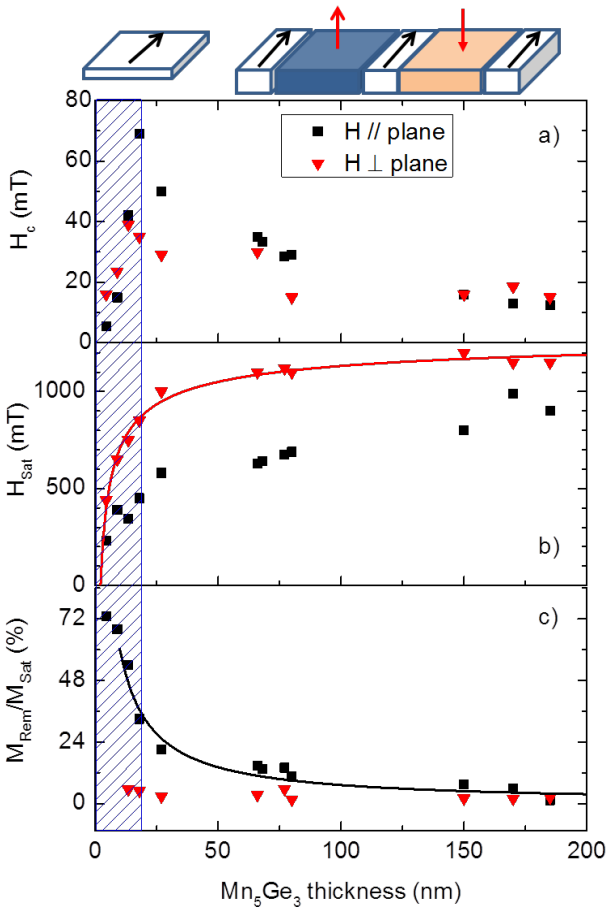

FIG. 3: (color online) Thickness dependence of parallel (black squares) and perpendicular (red triangles) (a) coercive field, (b) saturation field and (c) remanent magnetization. The hatched area corresponds to a domain state with predominantly in-plane magnetization. Above 20nm, the films exhibits a multidomain state with the out-of-plane magnetization pointing up and down as represented on the schematic drawing. Domains are separated by a Bloch-type domain wall.

plane from 0° to 180°. Whereas a six-fold anisotropy coming from the hexagonal structure of Mn_5Ge_3 crystal was expected, a two-fold symmetry has been measured. We have correlated this peculiar behavior with the magnetic history of the sample. The measurement has indeed been performed at 0.5 T coming from the positive saturation state, which has forced the magnetization in the DWs to align along the field direction. The six-fold in-plane magnetocrystalline anisotropy is consequently much weaker than the one induced by the domain walls.

Hysteresis curves have then been measured as the angle ϕ between the sample plane and external applied field varies from 0° to 90°. For increasing angles, the shape of the curves is gradually modified and characteristic features of the magnetization curves have been plotted in Fig. 5. As ϕ is increased, the remanent magnetization M_r progressively decreased from a maximum value to

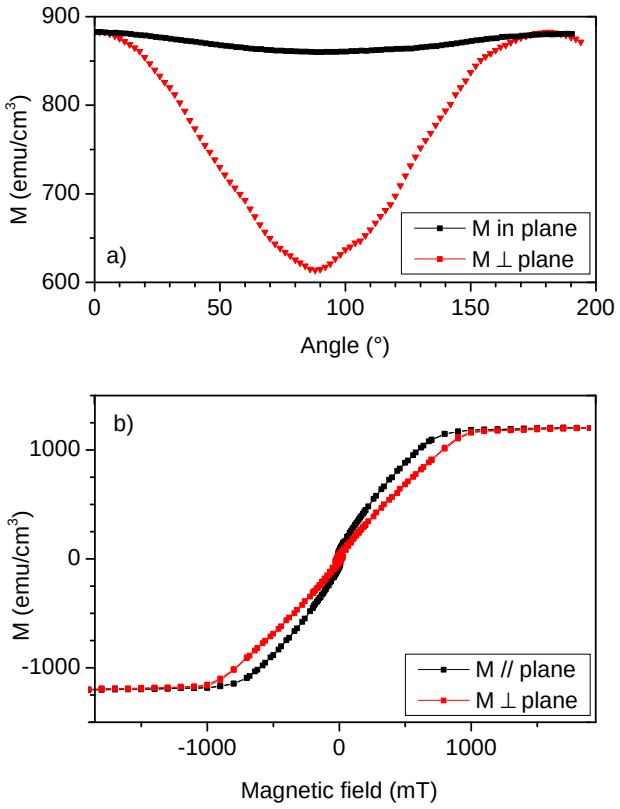

FIG. 4: (color online) Angular dependence of the magnetization of a 160 nm-thick sample in an 0.5 T field (a) as the latter is rotated in the sample plane, (b) as the angle ϕ between the applied magnetic field and the sample plane varies from 0° to 90°. All the measurements have been performed at 5 K.

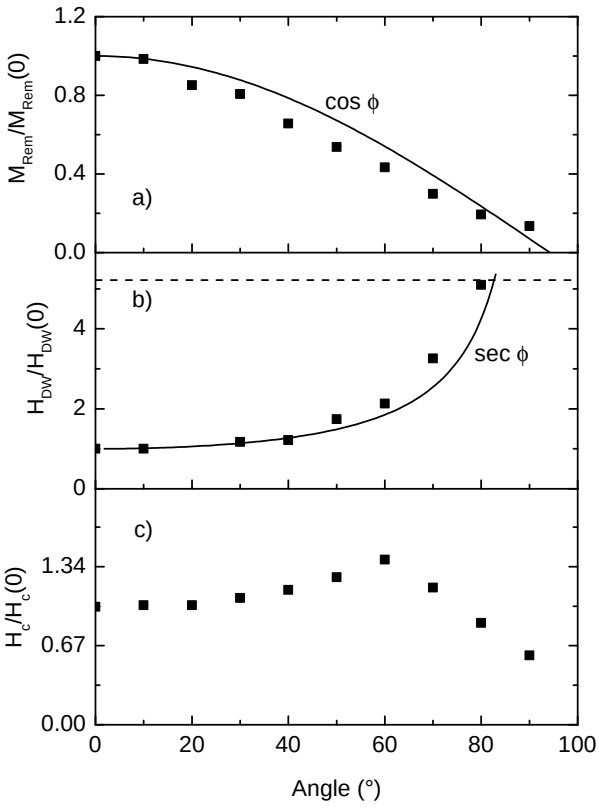

FIG. 5: Angular dependence of (a) the remanent magnetization and (b) the H_{DW} field corresponding to the end of the reversal in DWs. The dashed line represents the out-of-plane saturation field. (c) Angle variation of the coercivity. These values have been extracted from magnetic hysteresis loops performed on a 160nm-thick sample the angle ϕ between the applied magnetic field and the sample plane varies from 0° to 90°. All the parameters have been normalized to the values corresponding to $\phi = 0°$.

nearly zero. The cos ϕ dependence, corresponding to the in-plane projection, confirms that the remanent magnetization arises from the DWs.

We define as H_{DW} the value of the applied field for which the magnetization ends its non-reversible reversal. For increasing angle, H_{DW} increases monotonically from 0.2 to 1.1 T for $\phi \leq 80°$. A sec ϕ dependence fits very well the data up to this angle value as displayed in Fig. 5b, which indicates that switching in the domain wall occurs when the in-plane projection of the applied field reaches the critical value of 0.2 T. For $\phi = 90°$, no opening in the M-H curve is visible and a saturation field of 1.15 T, indicated in the figure by a dashed line, is necessary to align all the magnetic moments out-of-plane. This suggests that H_{DW} corresponds to the collective switch of in-plane magnetization direction within the domain wall and in the perpendicular configuration, no preferential in-plane orientation of the magnetization in DWs is present. When the applied field becomes less than $H_{Sat}^{\perp}$, small domains with opposite magnetization directions are nucleated but no anisotropy in DWs is present, which suggests that the domain structure is very different that the stripe structure present in the in-plane configuration. The prominent reversal mechanism in the out-of-plane configuration is therefore domain wall motion. On the other hand, in the in-plane field configuration, the magnetization switches direction at the DW center around the coercive field, then a coherent rotation of the out-of-plane magnetization present in the domains is necessary to confine all the magnetic moments in-plane. This means that stripe domains containing a small perpendicular component to the magnetization appear as soon as the applied field becomes inferior to $H_{Sat}^{//}$.

The coercive field has the unusual apparent behavior of first increasing with angle up to 60°, then decreasing with angle. This trend cannot be described using only a Stoner-Wohlfarth model of coherent rotation magnetization and we attribute this complex behavior results to a

change in the magnetic domain structure as the field direction varies between the in-plane to the out-of-plane direction. As an in-plane external field decreases from $H_{Sat}^{//}$ to zero, the magnetization in the domain goes through a coherent rotation without DW displacement because the latter oriented along the external field direction are not subjected to magnetic pressure from neither the applied field nor the demagnetizing field. In the DWs, the in-plane component remains parallel to the field direction in order to minimize Zeeman energy. The magnetization rotation plane is therefore defined by the direction of the applied field and the perpendicular direction to the surface. As a result, the domain structure is constituted of stripes oriented along the field direction. If the magnetic field is further decreased, a jump in the hysteresis loop corresponding to the collective switch of the magnetization in the DWs appears around the coercive field. On the other hand, when $\phi = 90°$, with the field applied perpendicular to the film plane, no sudden reversal is observed in the hysteresis curves. Coming from high-field saturation, domains with opposite magnetization are nucleated as soon as the applied field magnitude is decreased below $H_{Sat}^{\perp}$. As there is no preferential alignment direction for the magnetic moments in the DWs, a completely different domain structure is formed. Our results suggest that cylindrical magnetic bubbles with opposite magnetization have been nucleated since $H_{Sat}^{\perp}$ is well described by the Thiele's model. Such a magnetic structure has also been observed in Co[23] and Co-based alloys with perpendicular uniaxial anisotropy.[34] This structure is likely to evolve into elongated bubbles in interaction with each other around coercivity and this point will be developed in Sec.IV. However, no preferential in-plane anisotropy is introduced by this domain topology leading to low coercice fields. In conclusion, two well-defined magnetic structures can be observed: elongated bubbles for 90° and parallel stripes for $\phi = 0°$. During the transition between 90° and 0°, we restore an in-plane magnetic anisotropy and interstripe connections are possible leading to a more disordered magnetic structure. As a result the coercive field increases. Below 60°, the in-plane component prevails and the structure ought to gradually move to a stripe arrangement[35] leading to a decrease of the coercive field.

IV. DISCUSSION AND CONCLUSION

To conclude, this extensive study leads to a thorough description of both in-plane and out-plane magnetization reversals in Mn_5Ge_3 thin layers.

We first consider the case where the external magnetic field is applied in the film plane. Drawings in Fig.6 indicate schematically the domain structure of a 80-nm thick Mn_5Ge_3 thin film as the field is swept along the hysteresis loop. The dark blue and orange regions correspond to out-of-plane magnetization pointing up and down respectively. Domains with in-plane magnetization and domain walls are represented in white. By describing the hysteresis loop counterclockwise from high-field saturation, a weak-stripe domain structure (Fig.6b) appears as soon as the magnetic field becomes inferior to the saturation field above which all the magnetic moments points in the field direction (Fig.6a). As the applied field decreases, the perpendicular component of the magnetization increases because the applied field cannot overcome the magnetocrystalline anisotropy that forces the magnetization to lie along the normal to the sample plane. This reorientation occurs via a coherent rotation of the magnetic moment within each stripe. Without an applied field, the domain structure is made of stripes with perpendicular magnetization separated by domain walls in which the magnetization at the center of the wall is oriented along the direction of the initial applied field (Fig.6c). When the applied field is inverted and becomes negative, the magnetization within the domains starts to rotate in the field direction but the magnetization at the center of the domain wall stays in the plane and is now oriented oppositely to the applied field. At the coercive field, the magnetization in all the domain walls switches leading to a jump in the hysteresis curve (Fig.6d). The end of the magnetization cycle is obtained by coherent rotation of the domain magnetization in the applied field direction (Fig.6e and f).

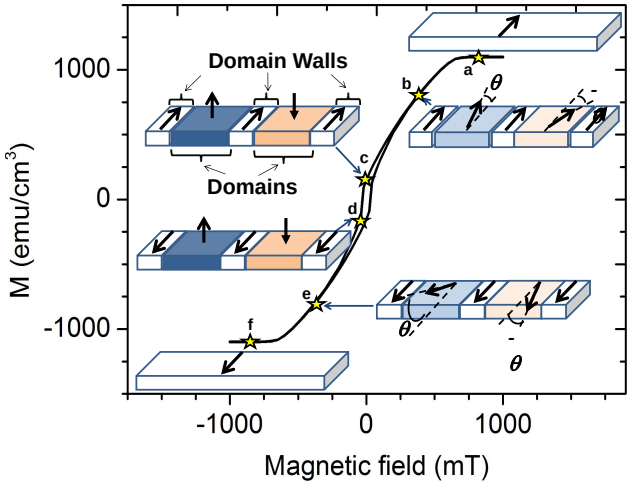

FIG. 6: (color online) Magnetization cycle of a 80 nm-thick Mn_5Ge_3 film obtained with the magnetic field applied in the sample plane. The drawings picture the domain structure for various field values.

The out-of-plane reversal of the same 80 nm-thick layer is presented in Fig.7. By describing the hysteresis loop counterclockwise from positive saturation field (Fig.7a), a characteristic opening of of the M-H curve appears around the saturation field. This singularity is the signature of domains with perpendicular magnetization and has been well studied.[36,37] Although direct imaging of the domains was not conceivable in this study due to the limited Curie temperature of the Mn_5Ge_3 compound, the data presented in this study are consistent with the model

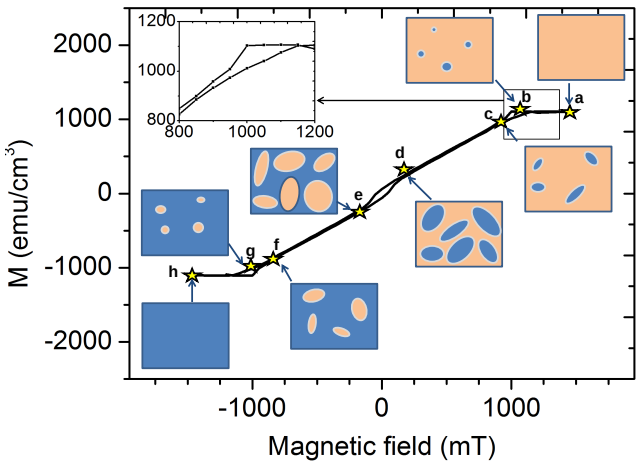

FIG. 7: (color online) Magnetization cycle of a 80 nm-thick Mn_5Ge_3 film obtained with the magnetic field applied perpendicularly to the sample plane. The drawings picture the domain structure for various field values.

described by Kooy and Enz[37]. This singularity has been ascribed to a sudden nucleation of magnetic bubbles in which the magnetization is oriented in the opposite direction (Fig.7b). The stability of the bubbles network has been studied by Thiele[28] who has shown that above a critical radius size, the bubble are inclined to form elliptic domains, which is the precursor step of stripes. By further decreasing the applied field, the domains with opposite magnetization (represented in dark blue in Fig.6) widen through domain wall motion leading to a quasi-linear variation of the magnetization with the applied field (Fig.7c and d). The presence of the demagnetizing field tends to stabilize the domain structure by opposing a magnetic pressure to the one imposed by the applied field and therefore slow down the domain wall motion. When the applied field is close to zero, the domain wall motion becomes more difficult because of repulsive interactions between opposite direction domains; the magnetization does therefore not follow a linear variation, which leads to a non-null remanent magnetization. For negative applied field, the dark blue domains connect to each other to give rise to orange elongated bubble through DW motion process (Fig.7e). This structure will then transform into cylindrical bubbles near negative saturation (Fig.7f and g).

In summary, Mn_5Ge_3 thin films with perpendicular anisotropy have been grown in a MBE chamber leading to very good crystalline quality. Using conventional magnetometry, we have studied the magnetization reversal process in Mn_5Ge_3 layers. We have identified a continuous reorientation of the magnetization from in-plane to out-of-plane for thicknesses comprised between 10 and 20 nm. Below 10 nm, the magnetization lies in-plane in a monodomain-type structure. Above 20 nm, the Mn_5Ge_3 layers exhibit a magnetic stripe structure. Interestingly, this critical thickness is much lower than the one found in materials with similar magnetic behavior. These boundary critical thicknesses, determined from careful data analyzes of hysteresis curves, are in excellent agreement with simple models calculations. Further quantitative data analyzes have lead to the determination of the magnetization saturation, the magnetocrystalline anisotropy constant, the exchange constant and the domain wall surface energy. All these results are strongly supported by theoretical calculations developed for uniaxial systems and the agreement of the two first quantities with literature is striking. This work has been concluded by a qualitative description of the magnetic reversal in Mn_5Ge_3 thin films. Low-temperature MFM measurements would be necessary to provide more quantitative characteristics such as domain sizes for instance. However, from our estimation, the size of the domains ought to be much smaller in Mn_5Ge_3 than in any conventional uniaxial thin films. Furthermore, the determined domain wall width is predicted to be smaller than the characteristic size of present day nanoelectronics devices and could lead to further miniaturization of domain wall devices. The features described in this paper emphasizes the potential applicability of Mn_5Ge_3 thin films for spintronics devices relying on magnetic switching and on controlled motion of domain walls by an external magnetic field and for the next-generation of data-storage devices. All these devices ought to be naturally compatible with the Si-based electronics.

* Electronic address: michez@cinam.univ-mrs.fr
† Present address: AIST, Tsukuba, Ibaraki 305-8568, Japan

[1] J.S. Tang, C.Y. Wang, M.H. Hung, X.W. Jiang, L.T. Chang, L. He, P.H. Liu, H.J. Yang, H.Y. Tuan, L.J. Chen, and K.L. Wang, ACS NANO **6**, 5710 (2012).
[2] J.S. Tang, C.Y. Wang, L.T. Chang, Y. B. Fan, T.X. Nie, M. Chan, W.J. Jiang, Y.T. Chen, H.J. Yang, H.Y. Tuan, L.J. Chen, and K.L. Wang, Nano Letters **13**, 4036 (2013).
[3] Changgan Zeng, Y. Yao, Q. Niu, and H. H. Weitering, Phys. Phys. Lett. **96**, 037204 (2006).
[4] M. A. Hamad, J. Supercond. Nov. Magn. **26**, 449453 (2013)
[5] T.F. Zheng and Y.G. Shi and C.C. Hu and J.Y. Fan and D.N. Shi and S.L. Tang and Y.W. Du, J. Magn. Magn. Mat. **324**, 4102 (2012)
[6] Changgan Zeng, S. C. Erwin, L. C. Feldman, A. P. Li, R. Jin, Y. Song, J. R. Thompson, and H. H. Weitering, Appl. Phys. Lett. **83**, 5002 (2003).
[7] D. D. Awschalom, and M. E. Flatté, Nature Physics 3, **3**, 153 (2007).
[8] A. Spiesser, I. Slipukhina, M.T. Dau, E. Arras, V. Le Thanh, L. Michez, P. Pochet, H. Saito, S. Yuasa, M. Jamet, and J. Derrien, Phys. Rev. B **84**, 165203 (2011).
[9] S. Picozzi, A. Continenza, and A.J. Freeman, Phys. Rev.

B **70**, 235205 (2004).
[10] Y.S. Dedkov, M. Holder, G. Mayer, M. Fonin, and A.B. Preobrajenski, J. Appl. Phys **105**, 073909 (2009).
[11] S. Olive-mendez, A. Spiesser, L.A. Michez, V. Le Thanh, A. Glachant, J. Derrien, T. Devillers, A. Barski, and M. Jamet, Thin Solid Films **517**, 191 (2008).
[12] P. De Padova, J.-M. Mariot, L. Favre, I. Berbezier, B. Olivieri, P. Perfetti, C. Quaresima, C. Ottaviani, A. Taleb-Ibrahimi, P. Le Fvre, F. Bertran, O. Heckmann, M.C. Richter, W. Ndiaye, F. D'Orazio, F. Lucari, C.M. Cacho, K. Hricovini, Surface Science **605**, 638 (2011).
[13] T. Nishimura, O. Nakatsuka, S. Akimoto, W. Takeuchi, S. Zaima, Microelectronic Engineering **88**, 605 (2009).
[14] J. M. Shaw, H. T. Nembach, and T. J. Silva, Phys. Rev. B **85**,054412 (2012).
[15] A. Spiesser, F. Virot, L.-A. Michez, R. Hayn, S. Bertaina, L. Favre, M. Petit, and V. Le Thanh, Phys. Rev. B **86**, 035211 (2012).
[16] A. Spiesser, S.F. Olive-Mendez, M.-T. Dau, L.A. Michez, A. Watanabe, V. Le Thanh, A. Glachant, J. Derrien, A. Barski, and M. Jamet, Thin Solid Films **518**, S113 (2010).
[17] Y. Tawara, and K. Sato, J. Phys. Soc. Jpn. **18**, 773 (1963).
[18] U. Gradmann, J. Magn. Magn. Mat. **54-57**, 733 (1986).
[19] M. Hehn, K. Ounadjela, S. Padovani, J.P. Bucher, J. Arabski, N. Bardou, B. Bartenlian, C. Chappert, F. Rousseaux, D. Decanini, F. Carcenac, E. Cambril, and M. F. Ravet, J. Appl. Phys. **79**, 5068 (1996).
[20] P. Bruno, J. Phys. F: Met. Phys. **18**, 1291 (1988).
[21] C. Kittel, Phys. Rev. **70**, 965 (1946).
[22] A.L. Sukstanskii, and K.I. Primak, J. Magn. Magn. Mat. **169**,31 (1997).
[23] M. Hehn, S. Padovani, K. Ounadjela, and J.P. Bucher, Phys. Rev. B **54**, 3428 (1996).
[24] V. Gehanno, Y. Samson, A. Marty, B. Gilles, and A. Chamberod, J. Magn. Magn. Mat. **172**, 26 (1997).
[25] V. Gehanno, R. Hoffmann, Y. Samson, A. Marty, and S. Auffret, Eur. Phys. J. B **10**, 457 (1999).
[26] N. Saito, H. Fujiwara, and Y. Sugita, J. Phys. Soc. Jpn. **19**, 421 (1964).
[27] N. Saito, H. Fujiwara, and Y. Sugita, J. Phys. Soc. Jpn. **19**, 1116 (1964).
[28] A.A. Thiele, Bell Syst. Tech. J. **50**, 725 (1971).
[29] N. Yamada, J. Phys. Soc. Jpn. **59**, 273 (1990).
[30] C Favieres, J Vergara, and V Madurga, J. Phys. Cond. Matt. **25**, 066002 (2013).
[31] D.M. Donnet, K.M. Krishnan, and Y. Yajima, J. Phys. D: Appl. Phys. **28**, 1942 (1995).
[32] D.J. Dunlop and O. Ozdemir, *Rock Magnetism: Fundamentals and Frontiers* Cambridge University Press, New York, 1997.
[33] F. Virot, L. Favre, R. Hayn and M. D. Kuz'min, J. Phys. D: Appl. Phys. **45**, 405003 (2012).
[34] C. Bran, A. B. Butenko, N. S. Kiselev, U. Wolff, L. Schultz, O. Hellwig, U. K. Rossler, A. N. Bogdanov, and V. Neu, Phys. Rev. B **79**, 024430 (2009).
[35] M. Demand, S. Padovani, M. Hehn, K. Ounadjela, and J. P. Bucher, J. Magn. Magn. Mat. **247**, 147 (2002).
[36] J.A. Cape, and G.W. Lehman, J. Appl. Phys. **42**, 5732 (1971).
[37] C. Kooy, and U. Enz, Philips Res. Rep. **15**, 7 (1960).